Journal of Applied Electrochemistry **33**: 613–617, 2003.

Electrochemical hydrogen permeation on steel sheets with *in situ* electrodeposition of a Pd layer at the exit side

L. PÉTER[1,*], E. SZŰCS[1], L. FILÁK[1], B. VERŐ[2] and H. SCHNEIDER[3]
[1]*Research Institute for Solid State Physics and Optics, Hungarian Academy of Sciences, H-1525 Budapest, PO Box 49, Hungary*
[2]*Bay Zoltán Foundation for Applied Research, Institute for Material Science and Technology, H-1509 Budapest, PO Box 53, Hungary*
[3]*Research and Quality Center Ltd, Brandenburg, Germany*
*(*author for correspondence, e-mail: lpeter@szfki.hu)*

Received 28 March 2002; accepted in revised form 24 March 2003

Key words: diffusion coefficient, hydrogen permeation, hydrogen trapping, Pd deposition, steel

Abstract

Electrochemical hydrogen permeation experiments were performed on Ti-microalloyed steel sheets. The input side was polarized as a cathode in a solution containing H_2SO_4 and $NaAsO_2$, while the solution at the exit side contained a concentrated NaOH solution with a minor amount of $Pd(NO_3)_2$. The presence of the palladium compound in the exit solution made it unnecessary to deposit an electrocatalytic Pd layer prior to the permeation experiments. Multistep permeation curves were recorded and the apparent diffusion coefficient of hydrogen, as calculated from the second breakthrough time, proved to be reproducible.

1. Introduction

Electrochemical hydrogen permeation has been a well-established experimental technique for more than forty years [1, 2]. In these experiments, one side of a metallic membrane serves as a cathode where hydrogen is evolved, and the exit side is polarized to be the anode where the hydrogen oxidation current is measured.

The flux of hydrogen entering the metal depends on the chemical composition and the microstructure of the metal sheet and on the applied current density. In the case of ferrous alloys, hydrogen entry promoters have to be applied to achieve an appreciable hydrogen flux. These promoters are mostly compounds of non-metallic elements like As, P and S, but metallic promoters as Th are sometimes also used [3]. Another alternative is the application of a Pd layer at the entry side [4].

The status of the exit side surface of the permeation membrane is crucial because the boundary conditions have to be well-defined for the quantitative analysis of the permeation curves. Permeation experiments with bare exit surface of the ferrous membrane without Pd coating usually lead to ill-defined permeation transients [5, 6]. However, the exit surface of the membrane can be coated with a Pd layer by sputtering [7, 8] or electrodeposition [4–6, 9–11] in order to ensure a sufficient electrocatalytic activity. The Pd layer has to be relatively thin as compared to the membrane to ensure that the hydrogen absorbed in the adlayer has no influence on the exit flux [6].

Several methods have been published about the electrodeposition of Pd onto different substrates [12], including iron or ferrous alloys [3, 9–11, 13]. Pretreatment of the substrate, composition of the Pd plating bath, deposition current density as well as the effect of the Pd layer thickness have been discussed in detail. The methods published all involve an *ex situ* palladium plating prior to permeation experiments.

The present work is motivated by the needs of the steel industry to characterize low-alloyed steel products before enameling. It is well known that the enamel coating can be damaged due to fishscaling [14] if the hydrogen penetrated into the metal during the enamel firing cannot be irreversibly bound. The current method for hydrogen absorption capability measurement in the enamel industry [15] yields only a blended parameter deducted from the first permeation transient, and hence this method does not allow one to determine the diffusion coefficient of the hydrogen and the concentration of hydrogen traps independently. However, there is great need for the determination of both the diffusion coefficient of hydrogen and trap concentration in a simple experiment.

In this paper, we present a method for hydrogen permeation measurement having three advantages.

Namely, (i) an electrochemical permeation device is employed; hence, the exit flux as a function of time is recorded (differential method); (ii) there is no need for Pd plating prior to the permeation experiment because a Pd layer is formed *in situ* and therefore the experiment can be carried in one step; and (iii) several subsequent transients can be observed in the permeation curves that makes it possible to determine the apparent diffusion coefficient of hydrogen independently of the trapping parameters.

2. Experimental details

A permeation cell made of Plexiglas was used with a chamber volume of about 85 ml. A round permeation window of 5 cm^2 surface area was cut out from the facing planes of the chambers. The sealing of the cell was ensured by silicone rubber o-rings along the edge of the permeation slit. All experiments were carried out at ambient temperature (23 $\pm$ 1 °C).

The thickness of the low-carbon steel sheets was 1.65 mm. Typical alloying and impurity levels (in weight percent) were: 0.24% Mn, 0.13% Ti, 0.056% Al, 0.027 % S, 0.011 % P, 0.011 % Si, <0.02% C (i.e., below the detection limit). The samples were IF (interstitial free) steel plates cold-rolled and annealed as usual. Structural investigation by using electron microscopy showed a ferritic microstructure with a typical grain size corresponding to ASTM no. 8. The specimens were either slightly polished with emery paper or used as received. In both cases, they were thoroughly degreased with ethanol before the cell was assembled. No pickling or etching was applied, and no acidic treatment was performed for the oxide layer removal in order to avoid the penetration of the hydrogen evolved during pickling into the specimen. These treatments are common in electrochemical hydrogen permeation studies for ferrous membranes [3, 5–7, 11], but in those cases the purpose is the measurement of the hydrogen diffusivity only, and the trap concentration is usually not of importance.

The composition of the input solution was 1.0 mol dm^{-3} for H_2SO_4 and 10^{-4} mol dm^{-3} for $NaAsO_2$. The As-content of the input solution also served as a corrosion inhibitor before the input side of the sample was polarized. In the conventional semi-electrochemical test [15], $HgCl_2$ is also used in the input solution to help to remove the oxide layer and to form a stable amalgam layer, but we intended to keep mercury absent for sake of environmental safety.

The input chamber was equipped with a Pt counterelectrode. At the input side of the permeation membrane, the cathodic current was controlled; hence no reference electrode was necessary. A Pt counterelectrode and a saturated calomel reference electrode (SCE) were immersed in the exit side solution, and the working electrode (i.e., the exit side of the membrane) was kept at a constant potential. All potentials cited below refer to the reference electrode. Solutions in both chambers were stagnant, and the oxygen was not expelled from the electrolytes.

A Keithley 225 current source was the current source for the input side, and an EF453 potentiostat (Electroflex, Hungary) provided the potentiostatic conditions at the exit side. The potentiostat was fully computer controlled, and the exit current against time data were also recorded by the computer.

3. Results

3.1. *Exit solution*

Several solution compositions were tested as a possible exit solution. It turned out that the dissolution or passivation current of the ferrous substrate remains high if the media is acidic (solute H_2SO_4), neutral (solute Na_2SO_4) or weakly alkaline (solute Na_2HPO_4). Hence, sodium hydroxide of 1–3 mol dm^{-3} concentration was applied.

$Pd(NO_3)_2 \cdot 2H_2O$ was applied as the source of the palladium to be deposited. Although $PdCl_2$ is less expensive than $Pd(NO_3)_2 \cdot 2H_2O$, the latter was used to keep corrosive anions absent. The strong alkaline solution of many palladium salts is stable [9], but the direct dissolution of the salts in concentrated NaOH solution is kinetically hindered [13]. Hence, the palladium salt was first dissolved in a dilute solution of sulfuric or phosphoric acid (c < 0.1 mol dm^{-3}), and the appropriate amount of this stock solution was poured into the NaOH solution. The resulting slightly yellow solutions were clean and stable over months. The contribution of the reduction of the Pd^{2+} content of the exit solution to the background current was typically -0.028 A cm^{-2} (mol $dm^{-3})^{-1}$.

In some cases, salts of organic acids were also added to the exit solution to facilitate the oxide layer removal from the permeation membrane. These additives had no substantial effect on the permeation experiments.

3.2. *Preconditioning of the exit surface*

After filling the exit chamber with the electrolyte, the potential of the working electrode was scanned between -0.4 and -1.1 V for 10–20 times. This pretreatment helped conditioning the electrode surface.

Steady-state cyclic voltammetric curves obtained at low sweep rate for the steel surface in 3 M NaOH solution and in the exit solution are shown in Figure 1. The current at the cathodic-going sweep is enhanced due to the Pd^{2+} addition, and the hydrogen evolution is much less hindered than in the absence of Pd^{2+}. The peak at the anodic-going sweep at -0.96 V (Figure 1) is due to the oxidation of the hydrogen atoms produced at more negative potentials. The properties of Pd could be observed even better if the sweep rate was high (500 mV s^{-1} or higher, see Figure 2). The potential of the exit side during the permeation experiment has to be

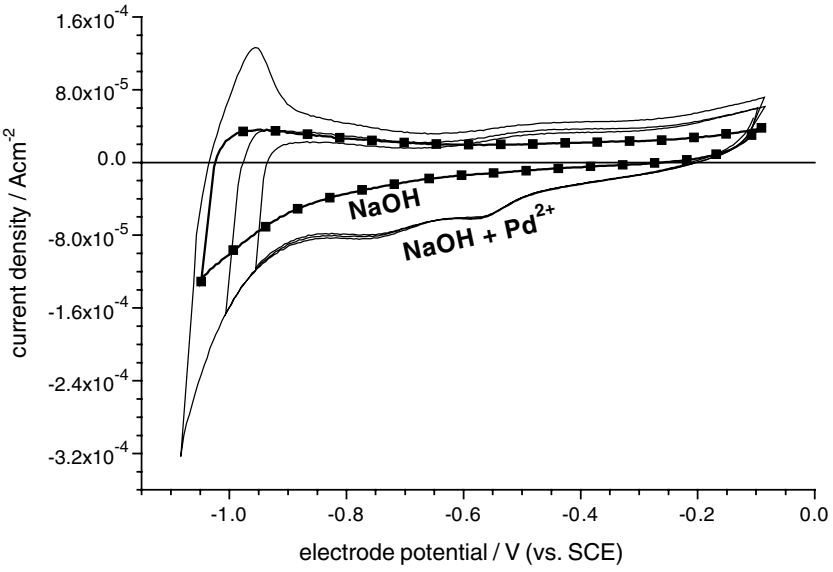

Fig. 1. Cyclic voltammetric curves obtained for IF steel permeation membrane. Parameters: c(NaOH) = 3.0 mol dm^{-3}; sweep rate 15 mV s^{-1}. Thick line with symbols, CV obtained in the absence of the palladium salt; thin line, CVs obtained with different cathodic limits when $c(Pd^{2+}) = 4 \times 10^{-4}$ mol dm^{-3}.

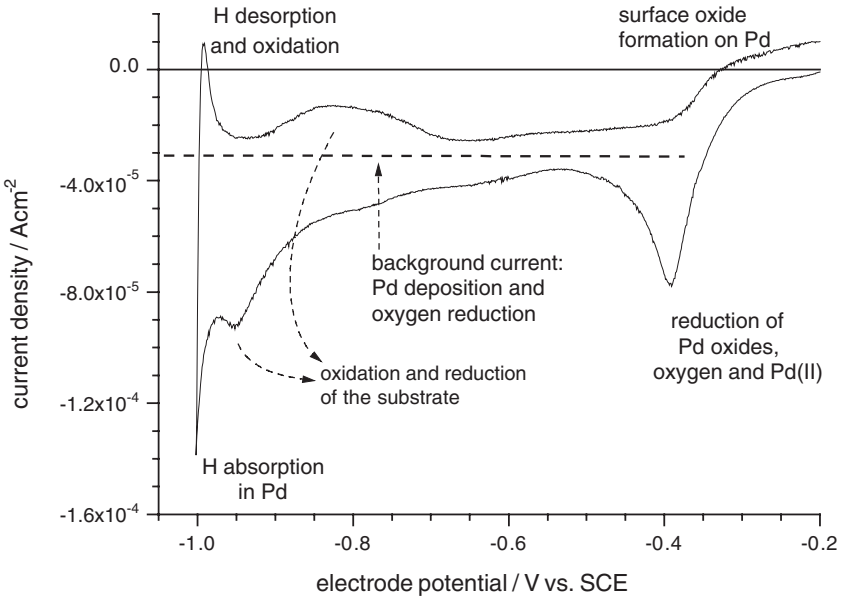

Fig. 2. Cyclic voltammetric curves obtained for IF steel permeation membrane. Parameters: sweep rate 500 mV s^{-1}, $c(Pd^{2+}) = 10^{-4}$ mol dm^{-3}, other condition as for Figure 1.

more positive than the H oxidation potential and more negative than the surface oxidation, that is, between −0.9 and −0.5 V. The Pd deposited under these condition is obvious because the shiny steel surface becomes dark black during the experiment. The presence of Pd at the exit side was also verified by a non-destructive electron probe microanalysis.

It was also found by other authors that such nano-Pd layers are very difficult to detect, but their presence at the exit surface makes the permeation effective and well-defined [11]. In our experiment, the monolayer coverage of the exit side was achieved during the preconditioning period, and the total thickness of the Pd layer at the end of the permeation experiment did not exceed 40 nm. Hence, the amount of the palladium deposited by *in situ* palladium plating was substantially reduced compared to previous *ex situ* palladium plating where the Pd layer thickness was 100 to 300 nm.

3.3. *Permeation experiments*

A typical multistep permeation curve obtained with *in situ* Pd deposition is shown in Figure 3. After an

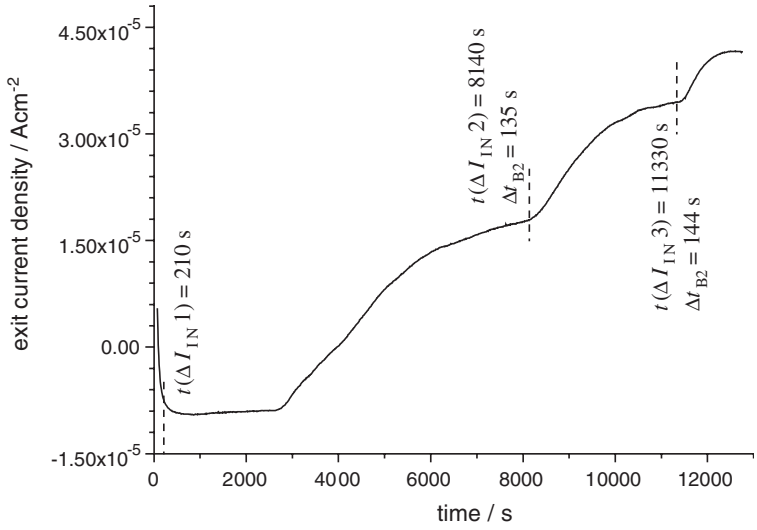

Fig. 3. Multistep hydrogen permeation curve recorded for a steel sample. Composition of the exit solutions: $c(\mathrm{NaOH}) = 3.0$ mol dm^{-3}, $c(\mathrm{Pd}^{2+}) = 10^{-4}$ mol dm^{-3}, $c(\mathrm{H_3C{-}COONa}) = 0.1$ mol dm^{-3}. Potential of exit side was −800 mV vs SCE.

initial current transient, the exit current varies very little with time and, therefore, a sufficient baseline (background current) can be established corresponding to the reduction of the dissolved O_2 and Pd^{2+}.

The advantage of the measurement of multistep permeation curves is that the traps are saturated during the first polarization period of the input side, and trap effects can no longer be observed if the input side current density is successively increased. (There is no agreement in the literature in whether the hydrogen can leave the traps when mobile hydrogen is no longer present [16, 17]). The increase in input side current also proved to be favourable because the input surface remained protected against corrosion.

The lowest input current density was 0.2 mA cm^{-2}. Hence, it can also be assumed that in the first polarization period the hydrogen absorbed does not generate additional traps [18].

3.4. *Evaluation method and diffusion coefficient of hydrogen*

The evaluation of the permeation curves was performed by using the concept of the breakthrough time Δt_B [19]. The first hydrogen breakthrough was observed some 1200–2600 s after the beginning of the hydrogen evolution at the input side. The first breakthrough time Δt_{B1} was the higher, the lower exit flux was observed at the end of the first permeation plateau. The current increase during the first permeation step is proportional to the input side hydrogen concentration and also to the input flux. It is obvious that the lower the input flux, the more time it is necessary to absorb enough hydrogen for the complete trap saturation. Thus, the dependence of Δt_{B1} with the steady-state permeation rate at the end of the first permeation step is well understood.

The second breakthrough time Δt_{B2} is determined by the apparent diffusion coefficient of hydrogen only if all traps are saturated by the time of the switch-on of the input current. Then, the usual relationship between the diffusion coefficient, D, and the breakthrough time can be applied: $D = d^2/(2\pi^2 \Delta t_{B2})$ where d is the sample thickness. The input side hydrogen concentration is taken as constant and the exit side hydrogen concentration is zero ([19], Equation 17). The apparent diffusion coefficients determined with the help of the second and further breakthrough times are shown in Figure 4. The apparent diffusion coefficients calculated are displayed as a function of the steady-state flux because different input side currents lead to different input side hydrogen concentrations and hence to different steady-state fluxes, and the diffusion coefficient may, in principle, also be a function of the hydrogen concentration. However, the data show that no trend can be established, but the scatter in the hydrogen diffusivity is due to either the experimental errors or the non-homogeneity of the samples. The latter factor may be significant because the samples were not chemically pure single crystal specimens but parts of an industrial product. Also, most of the steel samples studied in our laboratories with *ex situ* palladium coating showed some concentration-dependent hydrogen diffusivity. Hence, it is possible that a Pd layer plated *ex situ* changed the permeation conditions from a single layer problem to a bilayer problem [8].

The apparent diffusion coefficients measured differ from the lattice diffusion coefficient D_L in the sense that the apparent diffusion coefficient accounts not only for the effect of alloying atoms dissolved in the iron crystals but also for the influence of the inperfections in the structure, even if no entrapment takes place. This can be clearly seen from the difference in the lattice diffusion coefficients of hydrogen measured for pure well-annealed iron and the data shown in the present paper. Kiuchi and McLellan published $D_L = 7.2 \times 10^{-9}$ m^2 s^{-1} [22], while Bruzzoni et al. found $D_L = 9.6 \times 10^{-9}$ m^2 s^{-1}

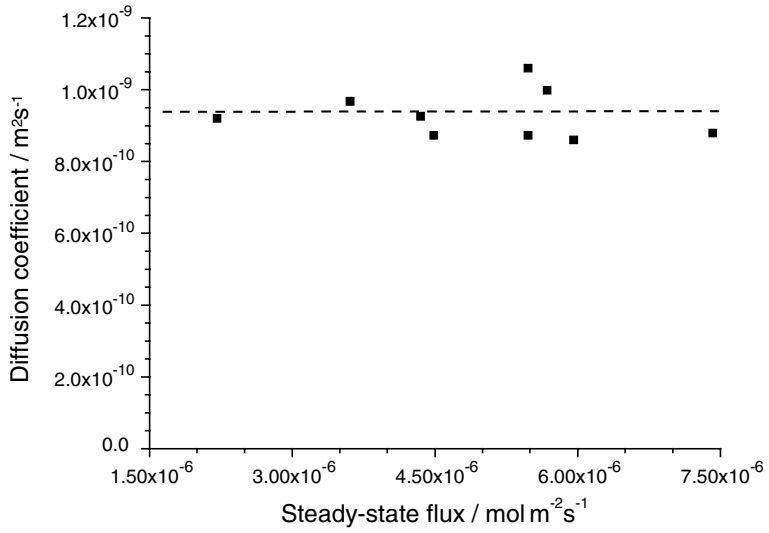

Fig. 4. Diffusion coefficient of hydrogen established for different IF steel specimens by means of the second and further breakthrough times of the permeation curves.

[6]. We obtained an apparent diffusion coefficient of 4.2×10^{-9} m^2 s^{-1} for polycrystalline ARMCO iron.

4. Discussion

The method presented makes it possible to measure hydrogen diffusivity and observe the first breakthrough time for samples that cannot be examined by means of the traditional semi-electrochemical hydrogen permeation method of the enamel industry. The need for a uniform hydrogen permeation method is generated by the variety of steel products recently commercialized. These steel types include, for instance, Ti-microalloyed interstitial-free (IF) steels or boron microalloyed steels. Ti and B are typical elements in whose presence the traditional semi-electrochemical hydrogen permeation method yields misleading results [15].

It has been shown by using digital simulation [20] that the kinetic factors of the hydrogen entrapment have a significant influence on the shape of the hydrogen permeation curves. The first breakthrough time, Δt_{B1}, is a function of the diffusion coefficient of hydrogen, the relative rate of the entrapment with respect to the diffusion, the ratio of the trap concentration to the input side hydrogen concentration and the steady-state saturation ratio of the traps. However, if the diffusion coefficient is measured for a specimen previously saturated with hydrogen, there is a chance that the fundamental parameters of hydrogen entrapment can also be determined from the first permeation transient.

The *in situ* palladium plating reduces the number of operations needed for a permeation experiment while maintaining the measurement accuracy. Therefore, the electrochemical permeation method can be made more suitable for routine industrial applications.

Acknowledgement

The authors thank Dr I. Bakonyi.

References

1. M.A.V. Devanathan and Z. Stachurski, *Proc. Roy. Soc.(London)* **A270** (1962) 90.
2. M.A.V. Devanathan, Z. Stachurski and W. Beck, *J. Electrochem. Soc.* **110** (1963) 886.
3. G. Zheng, B.N. Popov and R.E. White, *J. Electrochem. Soc.* **141** (1994) 1526.
4. J. Bowker and G.R. Piercy, *Metall. Trans. A* **16** (1985) 715.
5. P. Bruzzoni and R. Garavaglia, *Corros. Sci.* **33** (1992) 1797.
6. P. Bruzzoni, R.M. Carranza, J.R. Collet Lacoste and E.A. Crespo, *Electrochim. Acta* **44** (1999) 2693.
7. T-Y. Zhang, Y-P. Zheng and Q-Y. Wu, *J. Electrochem. Soc.* **146** (1999) 1741.
8. N. Takano, Y. Murakami and F. Teresaki, *Scr. Metall.* **32** (1995) 401.
9. T. Zakroczymski and Z. Szklarska-Smialowska, *J. Electrochem. Soc.* **132** (1985) 2548.
10. G. Zheng, B.N. Popov and R.E. White, *J. Electrochem. Soc.* **140** (1993) 3153.
11. P. Bruzzoni, R.M. Carranza and J.R. Collet Lacoste, *Electrochim. Acta* **44** (1999) 4443.
12. C.K. Lai, Y.Y. Wang and C.C. Wan, *J. Electroanal. Chem.* **322** (1992) 267.
13. P. Manolatos and M. Jerome, *Electrochim. Acta* **41** (1996) 359.
14. R. Valentini, A. Solina, L. Paganini and P. DeGregorio, *J. Mater. Sci.* **27** (1992) 6583.
15. Industrial standard EN 10209.
16. W-Y. Choo and J-Y. Lee, *Metall. Trans. A* **13** (1982) 135.
17. T. Zakroczymski, *J. Electroanal. Chem.* **475** (1999) 82.
18. J-Y. Lee and J-L. Lee, *Z. Phys. Chem.* **146** (1985) 223.
19. N. Boes and H. Züchner, *J. Less-Common Metals* **49** (1976) 223.
20. L. Péter, B. Almási, B. Verő and H. Schneider, *Mater. Sci. Eng. A* **339** (2003) 245.
21. W-Y. Choo and J-Y. Lee, *Metall. Trans. A* **14** (1983) 1299.
22. K. Kiuchi and R. McLellan, *Acta Metall.* **31** (1983) 961.